High gain - high power (HGHP) DC-DC converter for DC microgrid applications: Design and testing

B.Sri Revathi[1], M.Prabhakar[1*] and Francisco Gonzalez-Longatt[2]

[1] – School of Electrical Engineering, VIT University, Chennai, India-600127.

[2] – Centre for Renewable Energy Systems Technology – CREST, Loughborough University, United Kingdom.

* – Corresponding author, Associate Professor/School of Electrical Engineering,VIT University, Chennai, India – 600127. prabhakar.m@vit.ac.in, Tel: +91 44 3993 1154, Fax: +91 44 3993 2555.

Abstract

The use of green energy sources to feed DC microgrids is gaining prominence over traditional centralised AC systems. DC microgrids are characterised by the use of intermediate DC-DC converter which acts as power conditioning units. Hence, the choice of an appropriate DC-DC converter becomes significant as the overall system efficiency is strongly dependent on the converter's performance. This paper proposes a novel high gain high power (HGHP) DC-DC converter for DC microgrid, which is of one of the significant step forward in the development of DC microgrids. The suitability of the proposed HGHP DC-DC converter is demonstrated by experimental tests of the 60V/1.1kV, 3kW converter; test results validate the converter's suitability for DC distribution. A significant number of performance parameters of the proposed converter is compared with state of the art converter topologies demonstrating the superior capabilities of the proposed converter. This paper also portrays the potential benefits that could be reaped by trending towards DC instead of existing AC system. The advantages and challenges to be confronted in the foreseeable future while implementing sustainable DC microgrids are also highlighted. Finally, this paper encapsulates renewable energy fed DC microgrid system as an

appropriate, technically feasible, economically viable and competent solution for efficiently utilising the sustainable energy sources.

Keywords: Power electronics applications; Microgrid; DC-DC converter; Renewable energy integration; Distributed generation; High gain; Power conversion

1 Introduction

Electrical energy generated from fossil fuel sources is an option to fulfil the ever increasing load requirement. However, the process of electrical energy conversion from conventional energy sources (e.g. oil) pollutes the atmosphere leading to drastic and undesirable climatic fluctuations. The twin challenges of meeting the present day electrical energy demand while causing least damages to the environment are both massive and contradictory. Distributed renewable sources (DRSs) lend a great helping hand to confront this situation [1], [2]. Hence, among energy conscious planners, there is a significant inclination to efficiently convert and utilise electrical energy from the never exhausting, secure and non-polluting energy resources like solar, wind, etc [3],[4],[5]. Such a distributed renewable energy system should be simple, efficient, independent and stiff enough to replace the existing conventional system [6]. Moreover, the distributed renewable energy sources (RES) should possess desirable attributes: [7]

(i) Electricity energy storage facility [8];

(ii) Appropriate protection, monitoring and control mechanism;

(iii) Ability to operate in islanded and grid connected mode to ensure reliability;

(iv) Compatible with similar and other RES [9], [10] and

(v) Smart enough to prioritise the load demand based on supply availability [11].

The concept of a microgrid (μ-grid) is emerging as an excellent solution for interconnecting RES and the loads. [12]. The main advantage of microgrids, from the reliability point of view, is that they can operate in both islanded as well as grid connected mode [13], [14]. Residential, commercial, and/or industrial loads are connected to a microgrid. [15]. The overall performance of a microgrid system depends on the type of distribution used to supply the loads [16], [17]. As present day loads operate from AC supply, AC distribution continues to be in vogue for more than a century. Fig. 1 shows a general schematic representation of a typical conventional AC power system systems, the uni-directional power flow from generation to load is depicted.

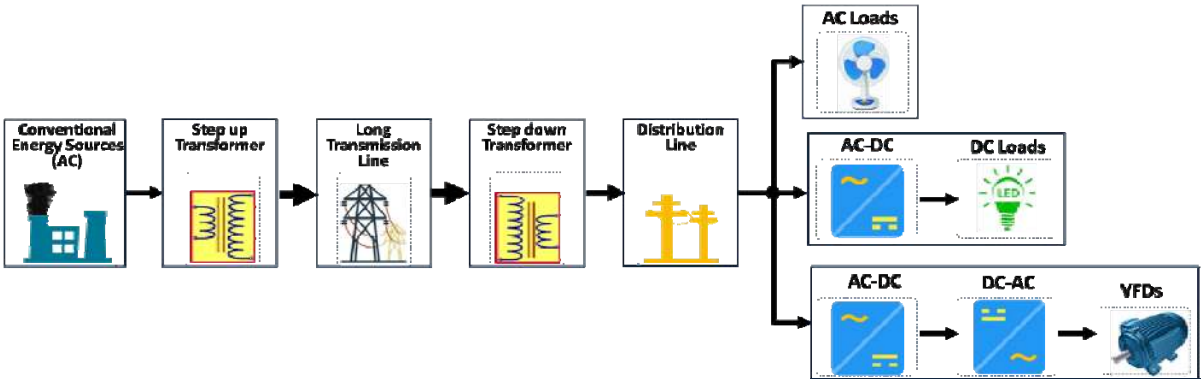

Fig. 1. Schematic diagram representing the main components of a traditional AC system.

The use of DC system on microgrid application is a realistic option. The DC distribution systems have good techno-economical potential compared to existing AC systems [18]. The use of low voltage DC (LVDC) has proven to be beneficial for the distribution networks [19]. LVDC is ideally suited for distribution networks due to its efficiency for shorter transmission distances and smaller transmission powers [20]. Also, DC distribution systems, particularly DC microgrids, make the grid more controllable, stable and reliable [21]. In DC distribution system, as capacitive leakage and inductive impedances do not exist in steady-state, higher power can be transferred with lesser voltage variation levels [22]. Further, like frequency, phase and reactive power requirements need not be considered in a DC microgrid, integrating many such DC microgrids to form a macro grid is simple. Therefore, planning, implementation and operation are simpler and less expensive [23].

Moreover, DC microgrids are more efficient than AC systems because:

(i) Certain energy-intensive manufacturing operations like smelting of aluminium, paper and pulp production units which waste more than 6% of total energy consumed in AC to DC conversion [24];

(ii) Data centres which operate at 10% higher efficiency, 20% less installation cost and 10% reduced equipment cost [25];

(iii) DC electrical loads such as LED lighting and electronic gadgets which are 20% of total electricity consumers in residential and commercial buildings [26];

(iv) Charging stations for electric vehicles, heating, ventilation and air-conditioning (HVAC) systems and various household appliances are well suited to DC power [27].

Fig. 2(a) shows the schematic diagram showing the general structure of a DC microgrid operating and the possibility of operating in grid-connected and off-grid mode. Various types of loads (critical and non-critical) connected to the DC microgrid are also clearly represented. Fig. 2(b) shows the schematic of a standalone DC microgrid feeding native DC loads and industrial variable frequency drives (VFD).

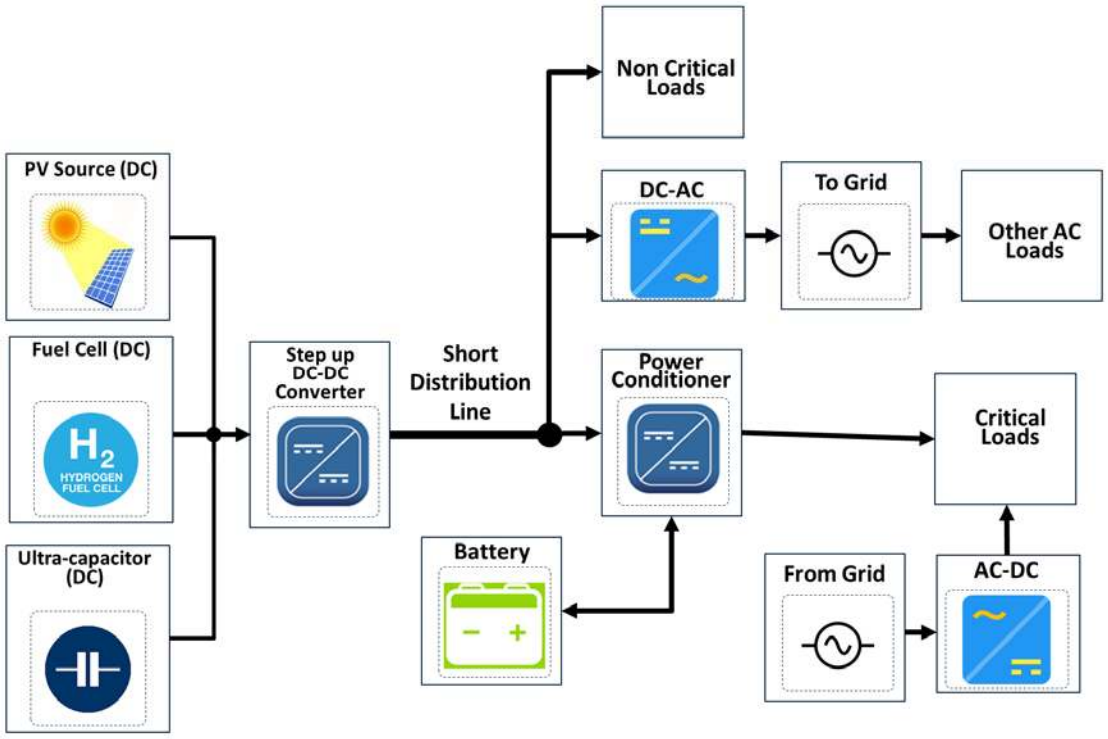

(a)

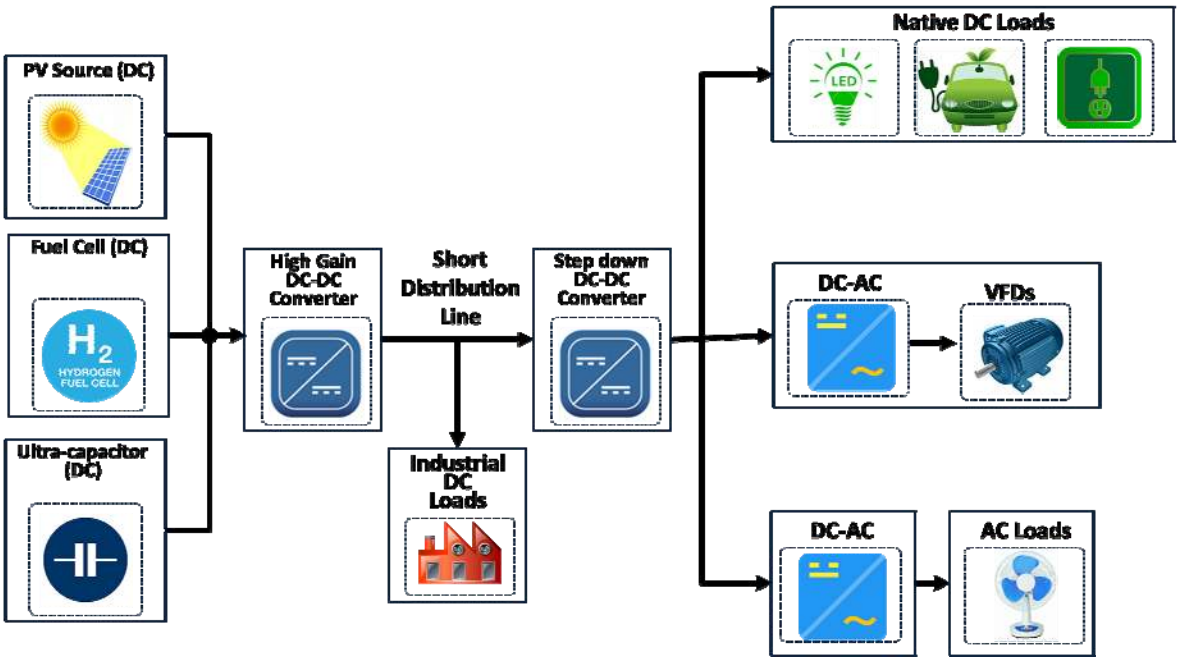

(b)

Fig. 2. Schematic diagram of a DC microgrid.

(a) Operating in grid-connected and off-grid mode.

(b) Operating in standalone mode.

Though it is extremely difficult and expensive to replace the present AC distribution system by DC, bypassing the existing AC grid and forming smaller DC microgrids is a viable alternative. The evolution could be like a DC layer overlapping the pre-existing AC layer. The evolution can be achieved by integrating RES with loads while avoiding unnecessary rectification and inversion stages are technically feasible as well as economically viable [28]. DC microgrids commendably integrate distributed generation sources, energy storage devices and a large variety of loads compared to AC microgrids.

Regarding social aspects, renewable energy fed DC microgrid is an affordable, more efficient, much faster and easier solution to demand and supply especially in rural areas [29]-[31].

In a DC microgrid, the crucial part of a DC distribution system is the DC-DC converter. To establish a competent renewable fed DC distribution system, proper selection and design of DC-DC converter with high voltage step up and high power handling capability is essential [32]. Other important features that motivate selection of a converter for DC distribution are discussed in [16] and [33].

For a RES fed DC distribution systems, a DC-DC converter capable of offering higher voltage step-up ratio is essential. Power distribution (in the range 2kW to 5kW) at 50V DC voltage level is inefficient due to higher cable loss. The higher voltage rating of the order of 1kV in the DC distribution system leads to smaller currents power losses compared to low voltage AC system [34]-[38].

According to EU low voltage directive (LVD 72/23/EEC), the use of 1 kV DC as a third distribution voltage level has proved to be a cost-efficient and effective solution to enhance the reliability of electricity distribution.

Conventional boost and boost derived converters are not suitable for high voltage gain applications as they suffer from practical issues like extreme duty ratio operation, large voltage stress on the switch, diode reverse recovery problems and poor efficiency [39]-[41]. Interleaved boost converters (IBC) are preferred for higher power ratings because of their inherent current sharing [42]-[44]. Non-isolated converters with appropriate gain extension techniques are preferred over isolated converters (which use transformers) mainly due to their merits like higher efficiency, reduced volume and size. Some of the commonly used gain extension methods are coupled inductor (CI) with and without IBC [45], [46], switched capacitor cells, voltage doublers [47], voltage multiplier cells (VMCs) [48] and charge pump technique. Though modular multilevel converters can cater to the high gain requirements, higher component count reduces their efficiency.

Active and passive voltage clamping are also employed in few converters to suppress the voltage stress on the power switches [49]. Some CI based topologies like winding cross-coupled inductors (WCCI), dual coupled inductor [50], switched coupled inductor, multi-winding [51] and multi CI based converters [52]-[54] are not very popular due to manufacturing complexity and larger switch voltage stress.

Switched-capacitor (SC) based converters alleviate the necessity of magnetic components resulting in compact and light power converters [55]. Unfortunately, the achievable voltage gain is only integral times the number of SC cells used. In [56], the high step-up conversion ratio is achieved by combining CI and SC. Voltage balancing of output capacitors which are located between adjacent SC cells is another tricky issue.

DC-DC converter topologies available in the literature are capable of offering either high voltage gain (>15) or handle large power levels (>1kW). Moreover, the existing DC-DC converters do not inherit many or few of the above-mentioned features which are vital for DC microgrids. Therefore, a most appropriate novel high gain high power DC-DC converter fulfilling most of the requirements of a DG fed DC microgrids is presented in this paper.

This paper proposes an extended version of a high gain high power (HGHP) converter which is presented in [57]. The proposed HGHP converter is one of the significant steps forward in the development of DC microgrids. The paper is organised as follows: Section 1 introduces the conceptual background and state of the art of high gain converters available in the literature, Section 2 describes the proposed HGHP topology, its operating principle and design details. Section 3 discusses the hardware tests and the results obtained. Section 4 presents the details regarding the converter performance which are compared with few existing converters. Sections 5 and 6 discuss the challenges and prospects of the proposed HGHP converter when employed in DC microgrids. Section 7 provides the concluding remarks.

2 Proposed HGHP DC-DC Converter

2.1 Topology Description and Operating Principle

Fig. 3(a) shows the power circuit diagram of the proposed converter. The converter structure comprises of two stages. Stage 1 is formed by a three phase IBC with the primary winding of three CIs, a voltage lift capacitor (C_{lift}) and a voltage lift diode (D_{lift}). The three legs of the IBC are operated with a uniform phase shift of 120° between them to reduce the input current ripple. C_{lift} and D_{lift} are used to multiply the voltage gain of the IBC by the number of interleaved phases. In Stage 2, each secondary winding of the CI acts as a voltage source to the VMCs formed by multiplier diodes (D_{M1}-D_{M6}) and multiplier capacitors (C_{M1}-C_{M6}). Three such arrangements are connected in series to extend the voltage gain. The rearranged version of Stage 2 is shown as an inset for clarity. Stage 1 and Stage 2 are cascaded through a diode (D_{IBC}) to prevent feedback of stored energy from the CIs. Diode D_0 acts as the classical boost rectifier diode while output capacitor C_0 is used to limit the output voltage ripple. This novel hybrid arrangement of CIs and VMCs enables this converter to yield higher voltage gain and handle higher power simultaneously. The operating modes are presented in [57]. Fig. 3(b) shows the characteristic waveforms of the proposed HGHP converter.

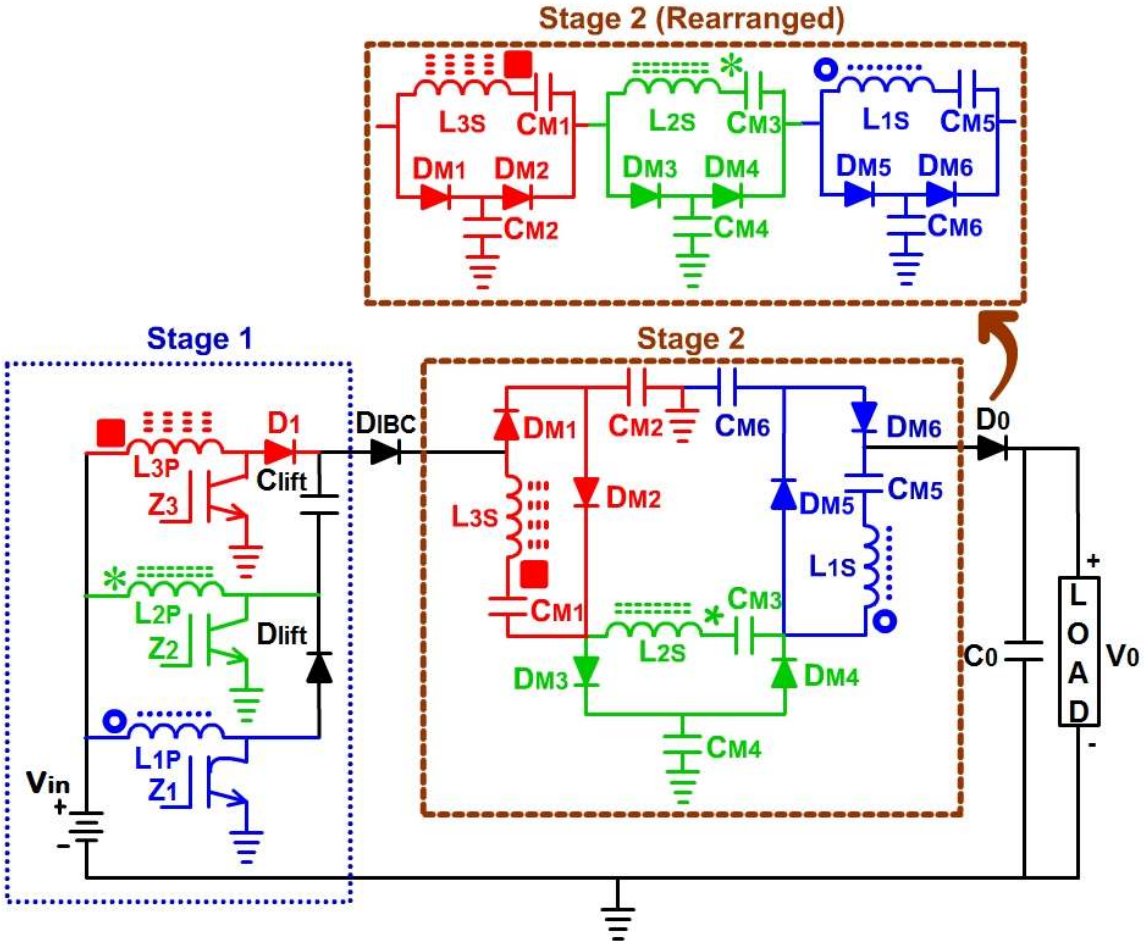
Stage 2 (Rearranged)
L3S
CM1
L2S
CM3
L1S
CM5
DM1
DM2
DM3
DM4
DM5
DM6
CM2
CM4
CM6
Stage 1
Stage 2
D1
DIBC
L3P
Z3
Clift
L2P
Z2
Dlift
L1P
Z1
Vin
+
-
DM1
CM2
CM6
DM6
D0
L3S
DM2
DM5
CM5
L1S
CM1
CM3
L2S
DM3
DM4
CM4
C0
V0
L
O
A
D
+
-

(a)

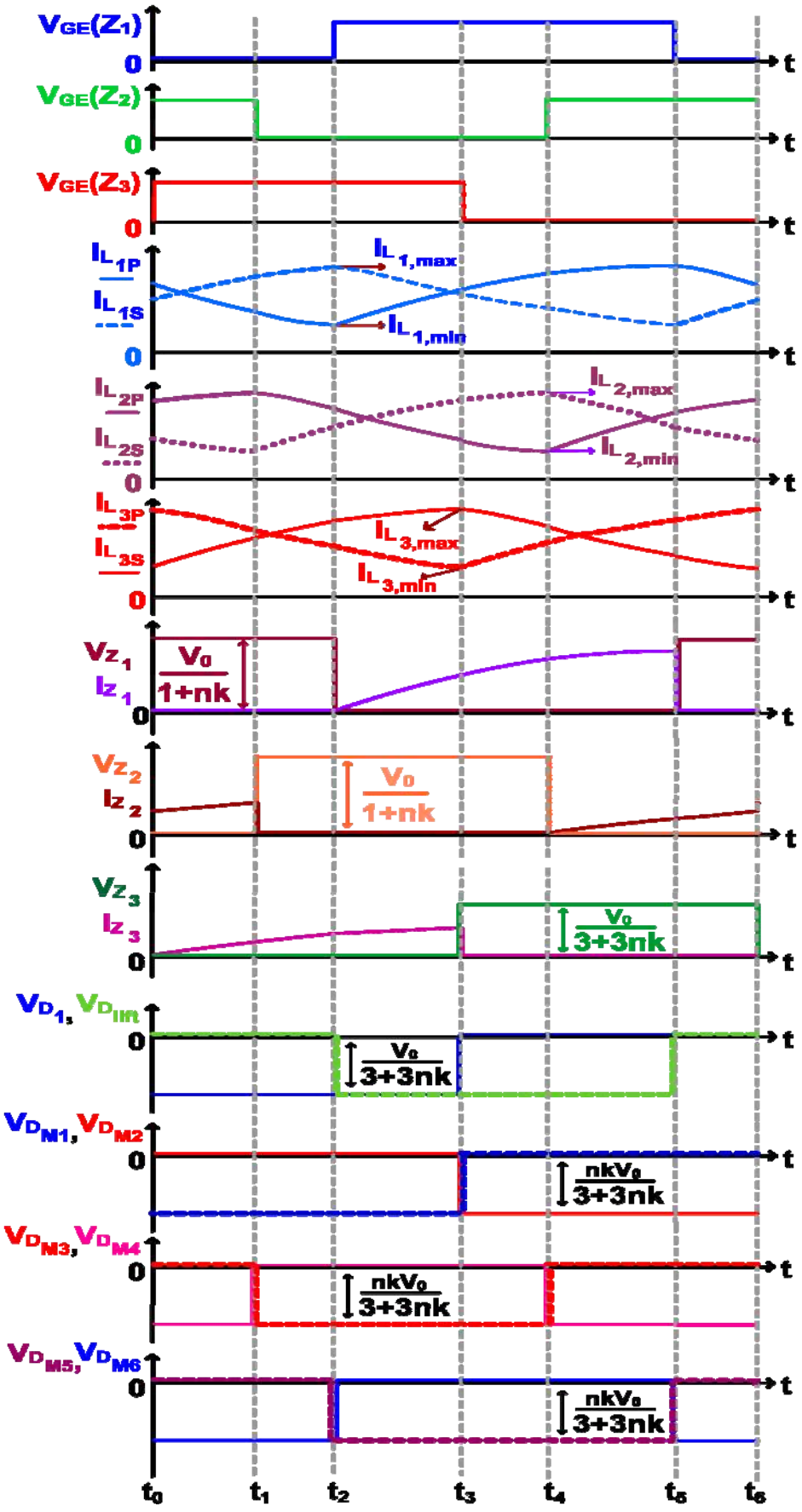
VGE(Z1)
VGE(Z2)
VGE(Z3)
0
t
IL1P
IL1S
IL 1,max
IL 1,min
IL2P
IL2S
IL 2,max
IL 2,min
IL3P
IL3S
IL 3,max
IL 3,min
Vz1
Iz1
Vo
1+nk
Vz2
Iz2
Vz3
Iz3
Vo
3+3nk
VD1, VD11n
VDN1, VDM2
nkVo
3+3nk
VDN3, VDM4
VDM5, VDM6
t0
t1
t2
t3
t4
t5
t6

(b)

Fig. 3. Proposed HGHP DC-DC converter for DC microgrids.

(a) Circuit diagram and (b) characteristic waveforms.

2.2 Steady State Analysis

This section is dedicated to analyse the proposed HGHP converter operating under the steady-state condition and derive key design details. Mathematical expressions describing important design parameters like (i) voltage conversion ratio, (ii) voltage and current stress across the semiconductor devices and (iii) passive elements are derived and presented.

2.2.1 Voltage Conversion Ratio

Stage 1 of the proposed converter is a three phase IBC. As voltage lift technique has been employed, the voltage gain of Stage 1 (V_{stage1}) is given by

$$V_{Stage\ 1} = V_{IBC} = V_{C_{lift}} = \frac{3}{1-D} V_{in} \tag{1}$$

where V_{IBC} is the voltage across the IBC stage, V_{in} represents the input voltage, $V_{C_{lift}}$ indicates the potential across C_{lift} with respect to ground and D represents the duty ratio of the switches.

Stage 2 of the proposed converter comprises of VMCs which are embedded with the secondary winding of each CI. Therefore, the voltage obtainable through Stage 2 (V_{stage2}) is

$$V_{Stage\ 2} = n\left(\frac{3k}{1-D}\right) V_{in} \tag{2}$$

where n represents the turns ratio of CI and k is the coefficient of coupling.

Using (1) and (2), the voltage gain (M) of the proposed converter is derived as

$$M = \frac{V_0}{V_{in}} = \frac{3(1+nk)}{1-D} \tag{3}$$

where V_0 is output voltage.

Generalising above shown approach, for a converter employing P number of interleaved phases (with P number of CIs each having n turns ratio with k being the coupling coefficient) and P number of VMCs, the overall voltage gain $M_{Generalized}$ can be deduced as:

$$M_{Generalized} = \frac{V_0}{V_{in}} = \frac{P(1+nk)}{1-D} \tag{4}$$

2.2.2 Switch Voltage Stress

Due to asymmetrical structure of Stage 1, voltage stress on the switches ($V_{Z_1}, V_{Z_2}, V_{Z_3}$) is different and expressed as

$$V_{Z_1} = V_{Z_2} = \frac{3}{1-D} V_{in} = \frac{V_0}{1+nk} \tag{5}$$

Switch Z_3 experiences a voltage stress similar to the switch present in a classical boost converter (CBC). Therefore,

$$V_{Z_3} = \frac{1}{1-D} V_{in} = \frac{V_0}{3(1+nk)} \tag{6}$$

Though the voltage stress on all the three power switches is unequal ($V_{Z1} = V_{Z2} \neq V_{Z3}$), the converter performance is not affected. All the three switches (Z_1, Z_2 and Z_3) are chosen with identical voltage rating for ease of fabrication.

2.2.3 Diode Voltage Stress

The diode D_1 is OFF when Z_3 conducts whereas diode D_{lift} is OFF when Z_1 is ON. Both D_1 and D_{lift} must be rated to block the voltage obtained from one interleaved phase. Therefore,

$$V_{D_1} = V_{D_{lift}} = \frac{1}{1-D} V_{in} \tag{7}$$

The voltage stress on D_{M1} ($V_{D_{M1}}$) is obtained when D_{M2} conducts. By applying Kirchhoff's Voltage Law (KVL) around the loop involving C_{lift}, D_{IBC}, D_{M1} and C_{M2}, the voltage stress is derived as

$$V_{D_{M1}} = V_{C_{M2}} - V_{C_{lift}} \tag{8}$$

$V_{C_{M2}}$ represents the voltage across C_{M2} and $V_{C_{lift}}$ indicates the voltage across C_{lift}.

The voltage across C_{M2} is given by

$$V_{C_{M2}} = V_{C_{lift}} + \left(\frac{nk}{1-D}\right)V_{in} \tag{9}$$

Substituting (9) in (8),

$$V_{D_{M1}} = \left(\frac{nk}{1-D}\right)V_{in} \tag{10}$$

From VMC concept, voltage stress on other multiplier diodes D_{M2}-D_{M5} is equal to (10). As D_{M6} is present closer to the output terminals, its voltage stress is minimum and same as the stress on D_0. Although voltage across adjacent multiplier cells increases steadily, the voltage stress on the multiplier diodes is equal. Therefore, diodes with identical voltage rating are used while fabricating.

2.2.4. Current Stress on Semiconductor Devices

Stage 1 of the proposed converter is asymmetrical due to the introduction of C_{lift}. The RMS value of currents flowing through Z_1, Z_2 and Z_3 are given by

$$I_{Z_1} = \frac{2}{3}I_{in}, I_{Z_2} = I_{Z_3} = \frac{1}{6}I_{in} \tag{11}$$

The RMS value of current stress on D_1 and D_{lift} will be same as the current through Z_3 and Z_1 respectively. Thus,

$$I_{D_1} = I_{Z_3} = \frac{1}{6} I_{in} \tag{12}$$

$$\mathrm{I_{D_{lift}}} = \mathrm{I_{Z_1}} = \frac{2}{3}\mathrm{I_{in}} \tag{13}$$

Since D_{IBC} and D_{M1} are present just after Stage 1, the current through them is

$$I_{D_{IBC}} = I_{D_{M1}} = \frac{1-D}{3} I_{in} \tag{14}$$

Since the multiplier diodes D_{M2}-D_{M6} are present in the gain extension stage, the RMS current through these diodes progressively decrease and are expressed as

$$I_{D_{M2}} = I_{DM3} = \frac{1-D}{3+nk} I_{in} \tag{15}$$

$$I_{D_{M4}} = I_{D_{M5}} = \frac{1-D}{3+2nk} I_{in} \tag{16}$$

$$I_{D_{M6}} = \frac{1-D}{3+3nk} I_{in} \tag{17}$$

The diodes D_{M6} and D_0 must be rated to carry the full load current I_0. Therefore,

$$I_{D_{M6}} = I_{D_0} = I_0 \tag{18}$$

2.2.5. Design of Passive Components

The proposed high gain high power (HGHP) DC-DC converter for DC microgrid is intended to be used in PV integration. The input current ripple of a DC-DC converter used in PV applications should be minimised to harness the maximum power from the input PV panels efficiently. While designing the inductor, a judicious trade-off is made between its size

and current ripple. For the CIs used in the proposed converter, the primary winding inductance ($L_{Primary}$) is determined from

$$L_{\text{Primary}} = \frac{V_{in}(V_{C_{lift}} - 3V_{in})}{3f\Delta i_L V_{C_{lift}}} \tag{19}$$

where f is the switching frequency and Δi_L represents the input current ripple.

The inductance value of the secondary winding is computed from the turns ratio n. The turns ratio is decided based on the required voltage gain and is expressed as

$$n = \frac{1}{k}\left[\frac{M(1-D)}{3} - 1\right] \tag{20}$$

The voltage across $C_{M1,}$ C_{M3} and C_{M5} is same as the voltage impressed across L_{3S}, L_{2S} and L_{1S} respectively. Since the three CIs have same turns ratio and coupling coefficient, voltage across these capacitors are same and given by

$$V_{C_{M1}} = V_{C_{M3}} = V_{C_{M5}} = \left(\frac{nk}{1-D}\right)V_{in} \tag{21}$$

The voltage across C_{M2} is given by (9). Each VMC cell contributes to a voltage gain given by (21). Therefore, voltage across C_{M4} and C_{M6} is deduced as

$$V_{C_{M4}} = V_{C_{M2}} + \left(\frac{nk}{1-D}\right)V_{in} \tag{22}$$

$$V_{C_{M6}} = V_{C_{M4}} + \left(\frac{nk}{1-D}\right)V_{in} \tag{23}$$

The output capacitor value C_0 is determined from duty ratio D, output current I_0, output voltage ripple ΔV_0 and the switching frequency f as

$$C_0 = \frac{DI_0}{f\Delta V_0} \tag{24}$$

3 Hardware Tests and Results

The proposed HGHP DC-DC converter suitable for DC microgrid applications has been implemented and then tested in order to demonstrate the suitability and the performance of the proposed concept. The hardware implementation is based on the parameters and specifications shown in Table 1. The gate pulses to switches Z_1, Z_2 and Z_3 are generated using TMS320F28027 digital signal processor (DSP). SCALE driver board 2AP043512 is used to interface the control and power circuit. The driver board and power module are kept in close proximity to reduce EMI issues. Tektronix makes TPS2024B digital storage oscilloscope (DSO) with four isolated channels along with standard accessories like P5210 high voltage probe, and A622 current probes are used to capture the key experimental waveforms. Fig. 4 shows the photograph of the experimental setup described above.

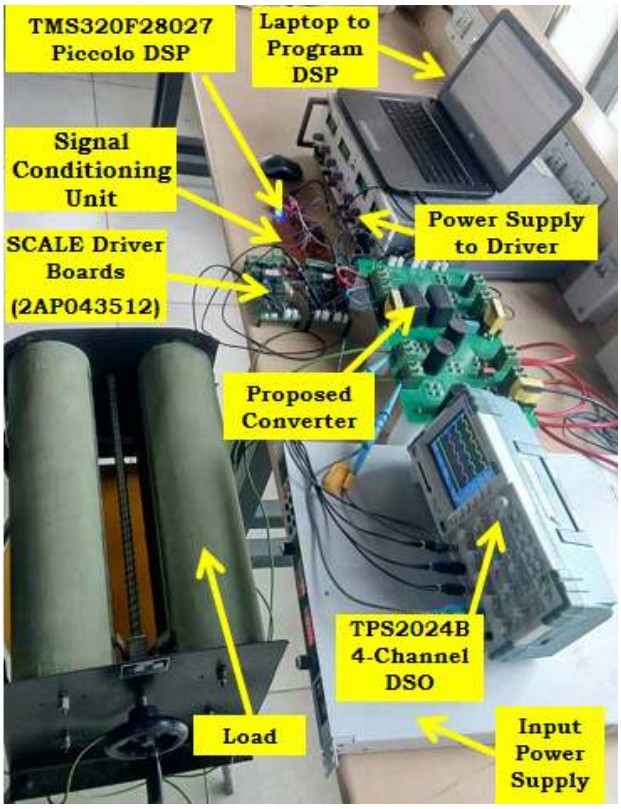

Fig. 4. Photograph showing the experimental setup of the proposed converter.

The first experimental test is performed to verify the high gain high power handling capability of the proposed converter considering a 60V input and 3kW load. Fig. 5(a) shows the experimental waveforms of the gate pulses (CH1-CH3) and output voltage, V_0 (CH4). The experimental measurements demonstrate the duty ratio, frequency and the phase shift between each pulse are fulfil the system requirement and specification defined in Table 1. Also, the experimental waveform of the output voltage exhibits a very low ripple as predicted from the design and specifications. The experimental results of the voltage waveforms in used to demonstrate the conversion ratio (18.3) of the proposed converter, and it is clear the requirements are properly fulfilled, the waveforms are presented in Fig. 5(b) and they perfectly match the theoretical value defined in the design stage.

Table 1. **Specifications of the main components of the proposed HGHP DC-DC converter for DC microgrid.**

Parameters	Specifications / Part Number
Input voltage, V_{in}	60 V
Output voltage, V_0	1.10 kV
Output power, P_0	3 kW
Switching frequency, f	100 kHz
Duty ratio, D	0.55
Turns ratio, n	2.0
Coefficient of coupling, k	0.875
Input ripple current	10% of input current (I_{in})
Primary coupled inductors: L_{1P}, L_{2P}, L_{3P}	18µH, 100kHz (L_{1P}-45A, L_{2P}-15A, L_{3P}-15A)
Secondary coupled inductors L_{1S}, L_{2S}, L_{3S}	72µH, 10A, 100kHz
Power switches Z_1, Z_2, Z_3 (IGBTs)	IXDN55N120D1 (1200V,100A, 2.3V)
Voltage lift diode, D_{lift}	VS-UFB280FA40 (400V, 170A)
Diodes D_1, D_{M1}	DSEI2X101-12A (1.2kV, 91A)
Diode D_{IBC}	DSEI2X101-06A (600V, 96A)
Diodes D_{M6}, D_0	DSS2X61-01A (100V, 60A)

Multiplier diodes D_{M2}-D_{M5}	DSEI2X31-06C (600V, 30A)
Capacitors C_{lift},C_{M2}	BC2799-ND (5µF/1.2kV)
Multiplier capacitors C_{M1}, C_{M5}	495-4186-ND (4.7µF/250V)
Multiplier capacitor C_{M3}	P14214-ND (4.7µF/450V)
Capacitors C_{M4}, C_{M6}, C_0	338-1376-ND (4.7µF/1.5kV)
Heat sink	294-1112-ND

Fig. 5(c) shows the experimental waveforms of the voltage across the capacitors at various key positions in the proposed converter. The waveform presented in CH1 shows the potential difference across C_{lift} while the remaining three channels (CH2, CH3 and CH4) demonstrate the voltage developed across C_{M2}, C_{M4} and C_{M6} respectively. Since C_{lift} is present between two interleaved phases, the voltage developed across C_{lift} is the voltage contributed by one IBC leg. The voltage built up across C_{M2}, C_{M4} and C_{M6} clearly validate the implemented gain extension concept. As the capacitor C_{M6} is located at the far end of Stage 2 and no further gain extension is envisaged, the potential across C_{M6} is same as the output voltage.

Fig. 5(d) shows the waveform of the current through the primary windings L_{1P}, L_{2P} and L_{3P} along with the input current, I_{in}. The total input current is shared among the three interleaved phases. As anticipated, the current distribution in the interleaved phases is unequal due to asymmetry. Since the switches are triggered with a uniform phase shift of 120°, the input current ripple is minimised. The magnitude of ripple current matches very closely with the designed value; the minor deviation (0.7 A) is attributed to the leakage present in the CIs.

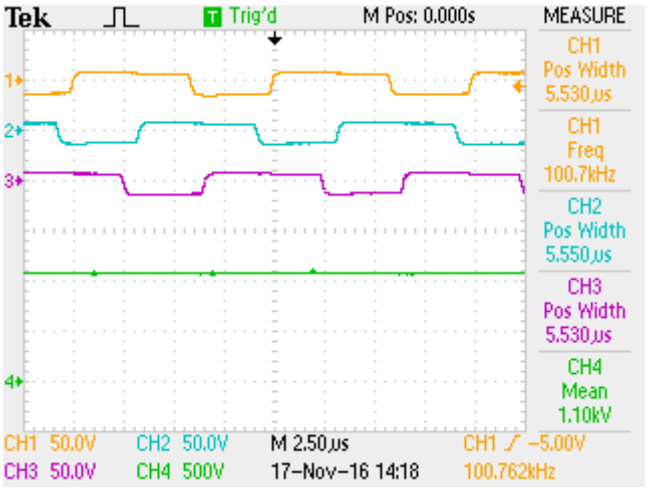

(a) CH1 – CH3(50V/div): Voltage across gate and emitter terminals (V_{GE}) of the power switches Z_1, Z_2 and Z_3 and CH4(500V/div): Output voltage. (Time scale 2.5µs/div)

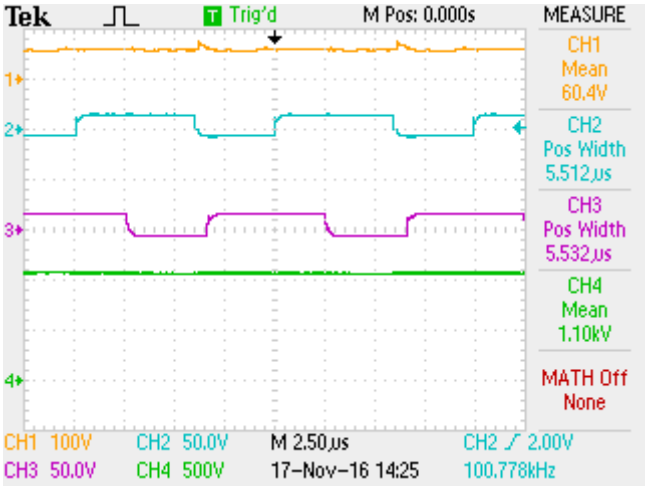

(b) CH1(100V/div): Input voltage, CH2 and CH3(50V/div): Gate pulses applied to switches Z_2 and Z_3, CH4(500V/div): Output voltage. (Time scale 2.5µs/div).

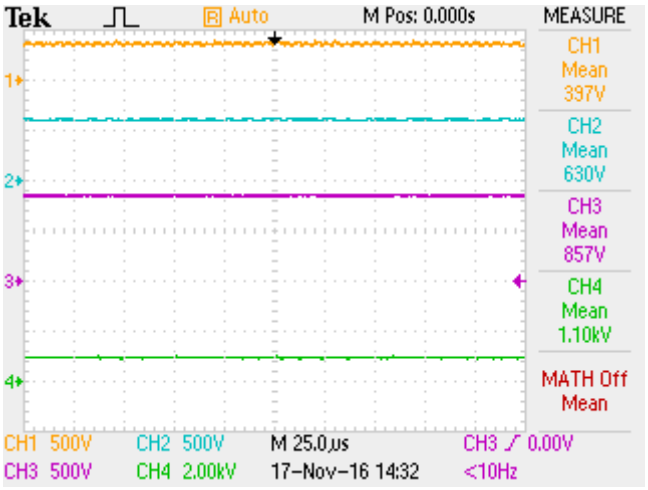

(c) CH1(500V/div): Voltage across C_{Lift}, CH2(500V/div): Voltage across C_{M2}, CH3(500V/div): Voltage across C_{M4}, CH4(2kV/div): Voltage across C_{M6}. (Time scale 25µs/div)

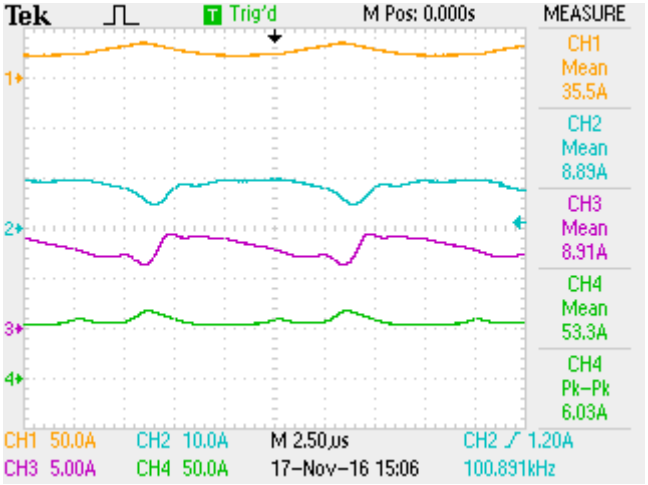

(d) CH1(50A/div), CH2(10A/div), CH3(5A/div): Current through L_{1P}, L_{2P} and L_{3P} respectively, CH4(50A/div): Input current I_{in}. (Time scale 2.5µs/div)

Fig. 5. Experimental results showing the voltage and current waveform captured using the oscilloscope: Test carried out at full load condition.

The second test on the proposed converter is conducted to determine (i) the voltage and current stresses experienced by the semiconductor devices at full load condition and (ii) the operating efficiency of the proposed HGHP converter when load varies from 75% to 115% of

full load. Fig. 6(a) shows the voltage stress on Z_3 as related to its gate pulse and the output voltage. The turn ON and turn OFF instants of Z_3 are in accordance with the applied gate pulse. The voltage stress on Z_3 is only about 12% of V_0. Despite of large voltage conversion ratio realised in this converter; the switch voltage stress is very low because (i) voltage gain extension occurs in Stage 2, and (ii) VMCs present in Stage 2 act as passive recycling network for transferring the stored energy in the leakage inductance to the load.

The waveforms presented in Fig. 6(b) to 6(d) pertain to efficiency computation at various load conditions. Under full load condition, the experimented converter operates at 92.63% efficiency. This efficiency value is acceptable since the converter simultaneously offers a high voltage gain of 18.3 and delivers 3 kW output power. The voltage reduction from the rated load to 115% of full load condition is about 50 V which translates to 4.54% voltage regulation at 89.78% efficiency. At 75% load condition, the voltage regulation is 8.63% while the efficiency is 90.10%. Energy storage elements contribute to a reasonably good voltage regulation even when operated under open loop mode. For DC microgrid, a constant DC bus voltage is needed to ensure proper operation of various loads connected to the common DC bus. When load condition tends to fluctuate, the energy storage elements used in the proposed HGHP converter act as energy buffer and maintain the DC bus voltage at the designed (specified) value. When operating at light load condition (75% of full load), the proposed converter yields a slightly higher voltage at the output. The output capacitor is rated to withstand this marginally higher output voltage. To maintain the DC output voltage at a constant and specified value and protect the other equipment/load connected to the common DC bus, duty ratio of the switches needs to be reduced slightly.

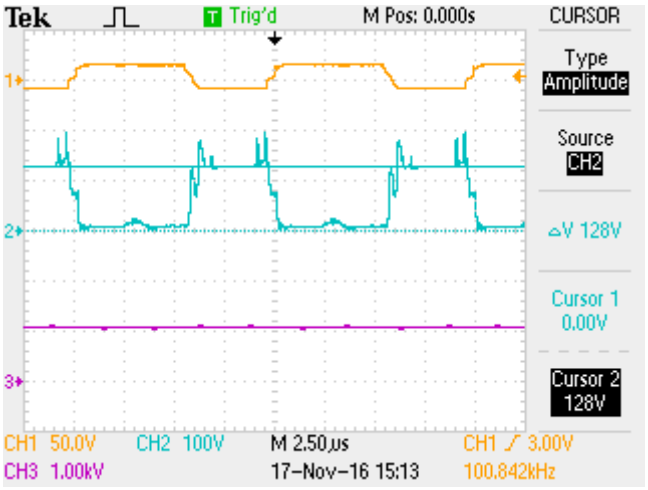

(a) CH1(50V/div): Gate pulse of Z_3, CH2(100V/div): Voltage stress on Z_3, CH3(1kV/div): Output voltage. (Time scale 2.5µs/div)

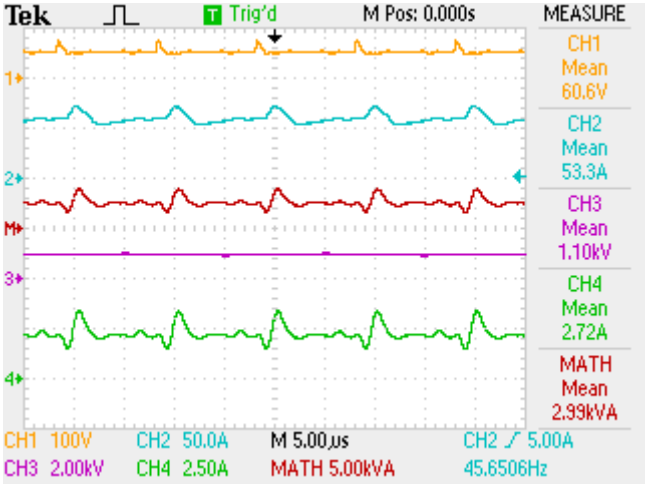

(b) CH1(100V/div) and CH2(50A/div): Voltage and current at the input terminals respectively, CH3(2kV/div) and CH4(2.5A/div): Voltage and current at the output, MATH(5kVA/div) (channel 'M'): Output power at full load. (Time scale 5µs/div).

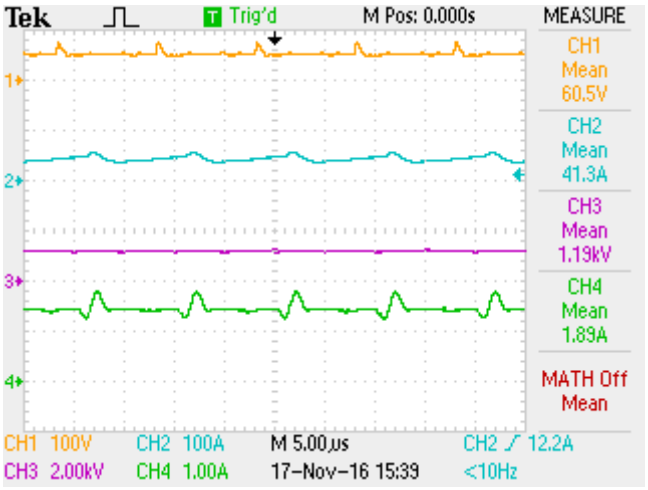

(c) CH1(100V/div), CH2(100A/div), CH3(2kV/div) and CH4(1A/div): same as Fig. 6(b) at 75% of full load. (Time scale 5µs/div)

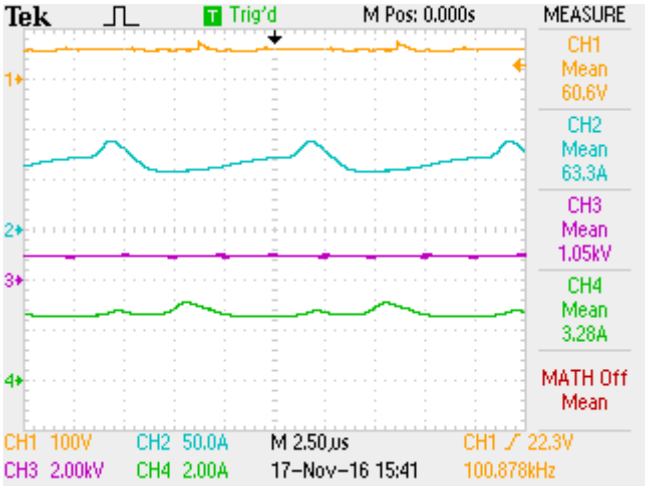

(d) CH1(100V/div), CH2(50A/div), CH3(2kV/div) and CH4(2A/div): same as Fig. 6(b) at 125% of full load. (Time scale 2.5µs/div)

Fig. 6. Experimental results showing the voltage and current waveform captured using the oscilloscope: Test carried out at full load condition.

The loss distribution of the converter under full load condition is calculated from (24)-(26).

$$P_{switch\_loss} = I^2_{switch\_RMS} \times R_{switch\_ON} + P_{switch\_ON} + P_{switch\_OFF} \quad (24)$$

$$P_{diode\_loss} = V_{diode\_ON} \times I_{diode\_Avg} + I^2_{diode\_RMS} \times R_{diode} \quad (25)$$

$$P_{CI\_loss} = I_{py}^2 \times R_{py} + I_{sy}^2 \times R_{sy} + P_{iron} \quad (26)$$

where

P_{switch_loss}, P_{diode_loss}, P_{CI_loss} and P_{iron} are the power loss occurring in the switches, diodes, coupled inductor and magnetic/ferrite core of CI respectively.

P_{switch_ON} and P_{switch_OFF} are respectively the turn ON and turn OFF power loss occurring in the switches.

I_{switch}, I_{diode}, I_{py} and I_{sy} are the current flowing through switch, diode, primary winding of CI and secondary winding of CI respectively.

R_{switch}, R_{diode}, R_{py} and R_{sy} are the resistance of the switch, diode, primary winding and secondary winding of CI respectively.

From the manufacturers' datasheet, the required parameters like R_{switch_ON}, R_{diode} and P_{iron} are obtained and the respective losses are calculated. Fig. 7shows the loss distribution of the converter under full load condition. The conduction loss and switching loss occurring across the power switches account for about 45% of the total losses. Generally, polypropylene capacitors are efficient and contribute to very low losses. To minimise the losses occurring across the connecting wires, thick stranded conductors with low resistance is used. Thick multi-layered printed circuit board (PCB) tracks are used to reduce the losses occurring across them. Overall, the losses occurring across the capacitors, losses occurring in the PCB, connecting wires, etc. are minimal and work out to 2% of the total power.

Fig. 8 shows the top view photograph of the implementation of the proposed converter laid on the PCB. Modules with SOT227 package are used as power switches and diodes. The coupled inductors operate at the 100ckHz frequency and are wound using litz wire to reduce conduction losses, size and volume. Consequently, the three CIs are conveniently

accommodated on the PCB itself. Switches and diodes are naturally cooled using individual peel and stick type heat dissipators. Fig. 9 shows the front view photograph of the assembled converter. Capacitors C_{M4}, C_{M6} and C_0 were the tallest components with a height of about 0.065 m. The overall dimensions of the converter are 0.385m × 0.230m × 0.065m (length × width × height).

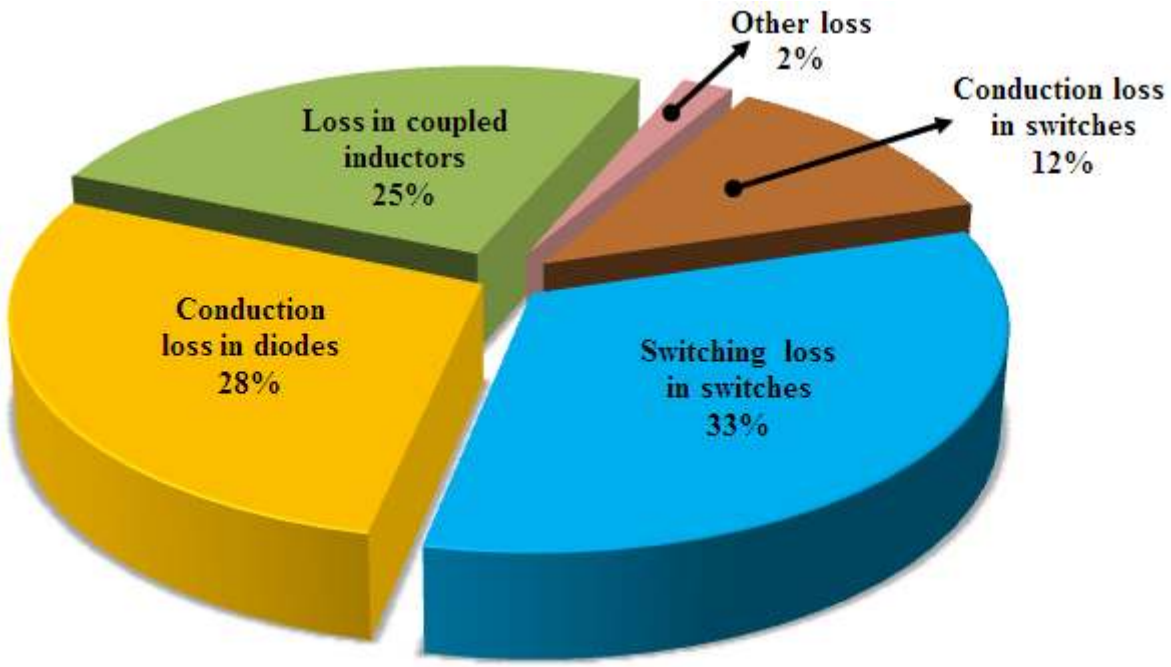

Fig. 7. Loss distribution of the experimented converter operating at rated condition.

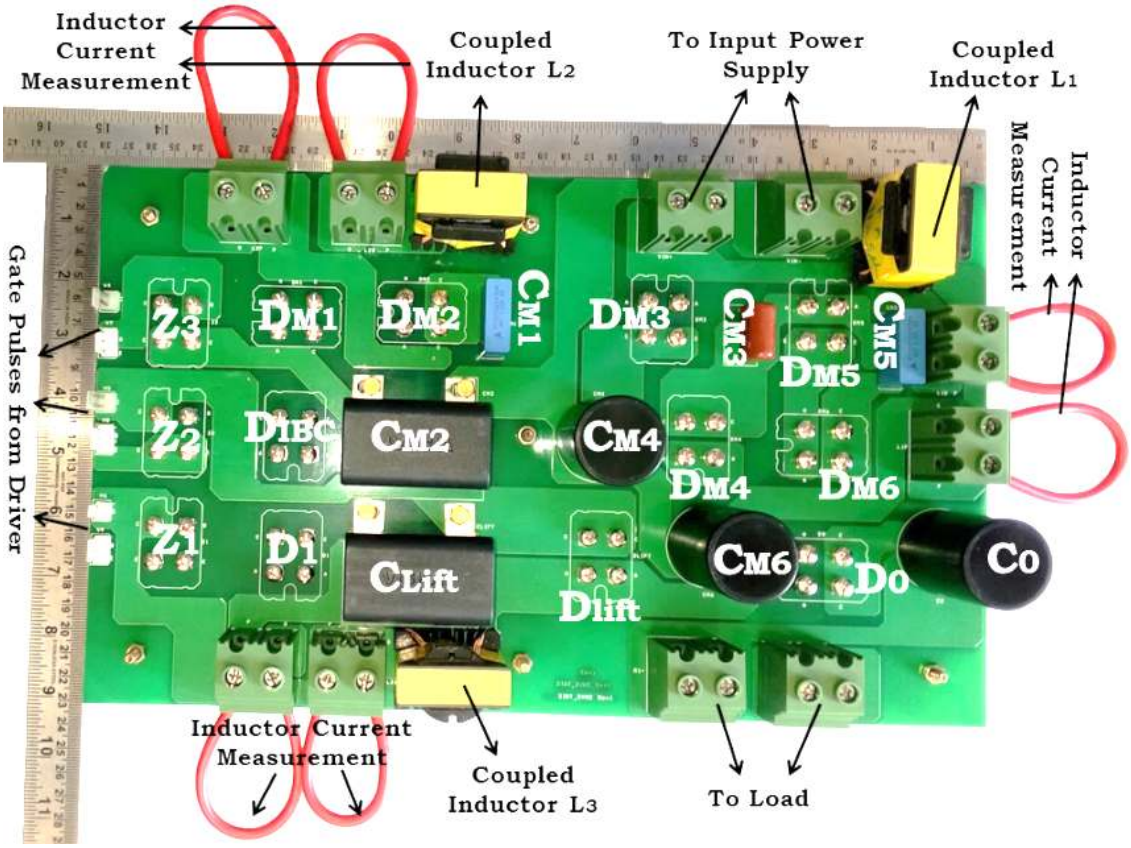

Fig. 8. Photograph showing the top view of the implemented HGHP DC-DC converter for DC Microgrids.

Fig. 9 Front view photograph of the proposed HGHP converter.

4 Performance Analysis and Comparison with Few Existing Converters

The performance of the presented HGHP DC-DC converter suitable for DC microgrid applications is evaluated considering variations in turns ratio (n), the duty ratio (D), the coefficient of coupling (k) of CIs and load conditions, simulation results are presented below.

4.1 Efficiency and Output Voltage

Fig. 7(a) shows the output voltage and efficiency values at various load conditions obtained during simulation and experimentation for the HGHP DC-DC converter suitable for DC microgrid applications. The peak operating efficiency of the converter is about 92% under full load condition. When the load varies from 75% to 115% of rated load, the practical efficiency fluctuates within a narrow 3% band. This narrow fluctuation is an advantage, and due to the presence of energy storage elements which ensure appropriate delivery of demanded output power over the load range considered. The output voltage remains almost constant over a load variation ranging from 75% to 115% of full load and proves the voltage gain capability of the converter while validating the design hypothesis.

Fig. 10(b) shows the plot of ideal voltage gain (k = 1) versus duty ratio variation for the adopted and few existing converters. Proposed HGHP DC-DC converter offers the highest voltage gain compared to other converters. Converter presented in [47] and [55] offer the same gain as turns ratio is unity for this converter. Fig10(c) shows the voltage gain variation of the proposed converter with variation in turns ratio n. The desired operating point is achieved at n = 2 and k = 0.875 (experimentally determined value). Since CIs are used in the proposed converter, its voltage gain varies as the coupling coefficient varies. This variation is shown in Fig. 10(d). The change in voltage gain at a particular duty ratio when k varies from 0.875 to 1 is very less and proves that the variation in k does not drastically affect the practical output voltage.

4.2. Voltage Gain and Power Handling Capability

To appreciate the advantageous features of the proposed HGHP DC-DC converter, its main attributes are benchmarked with converters presented in [52], [53], [55] and [56]. Table 2 provides some important attributes which are compared. All the converters that are compared provide a voltage gain of more than ten except the converter in [53], whose voltage gain is 9.83. Converters presented in [52], [53] and [55] use two CIs with a relatively smaller turns ratio of 1 and 1.6 in [52]. Though the voltage gain of converters is higher than 10 (except [53]), their power handling capability is limited to 1 kW mainly due to the gain extension technique adopted. In the proposed converter, the presence of IBC as its first stage with three CIs enables the converter to handle 3 kW power at the desired voltage level.

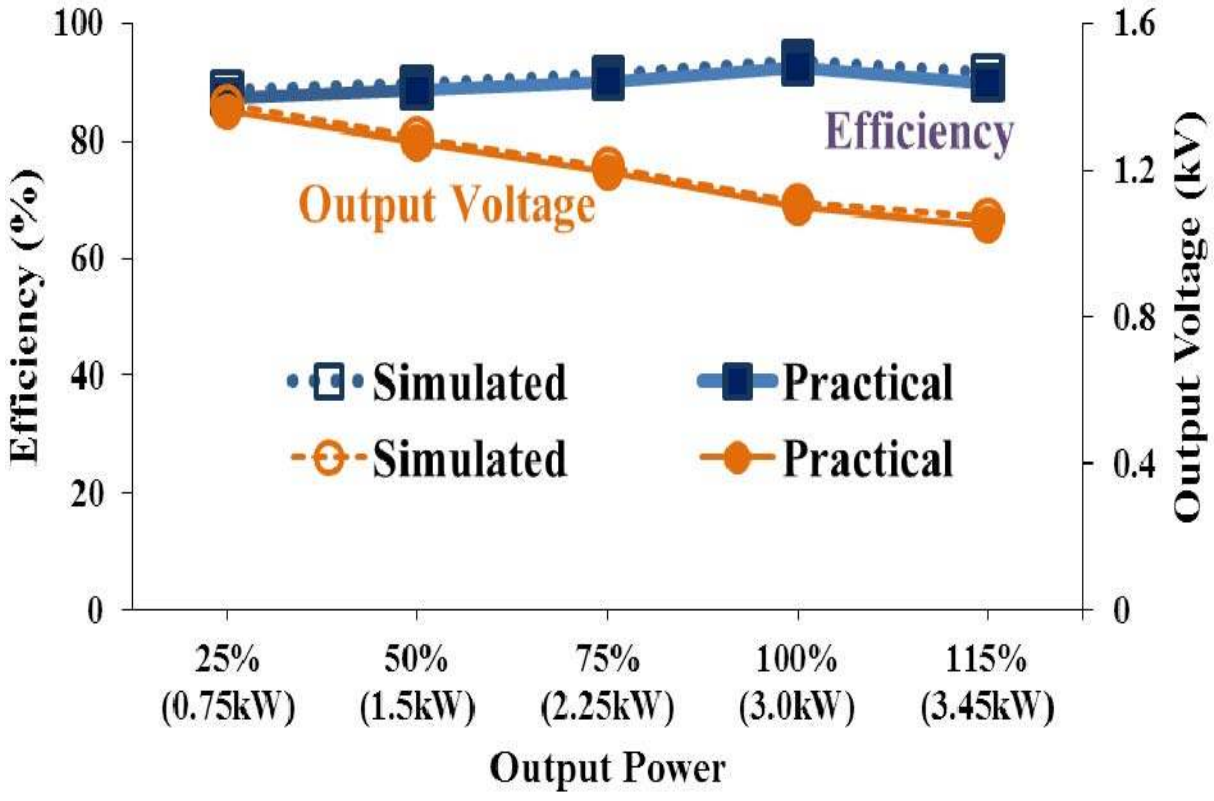

(a)

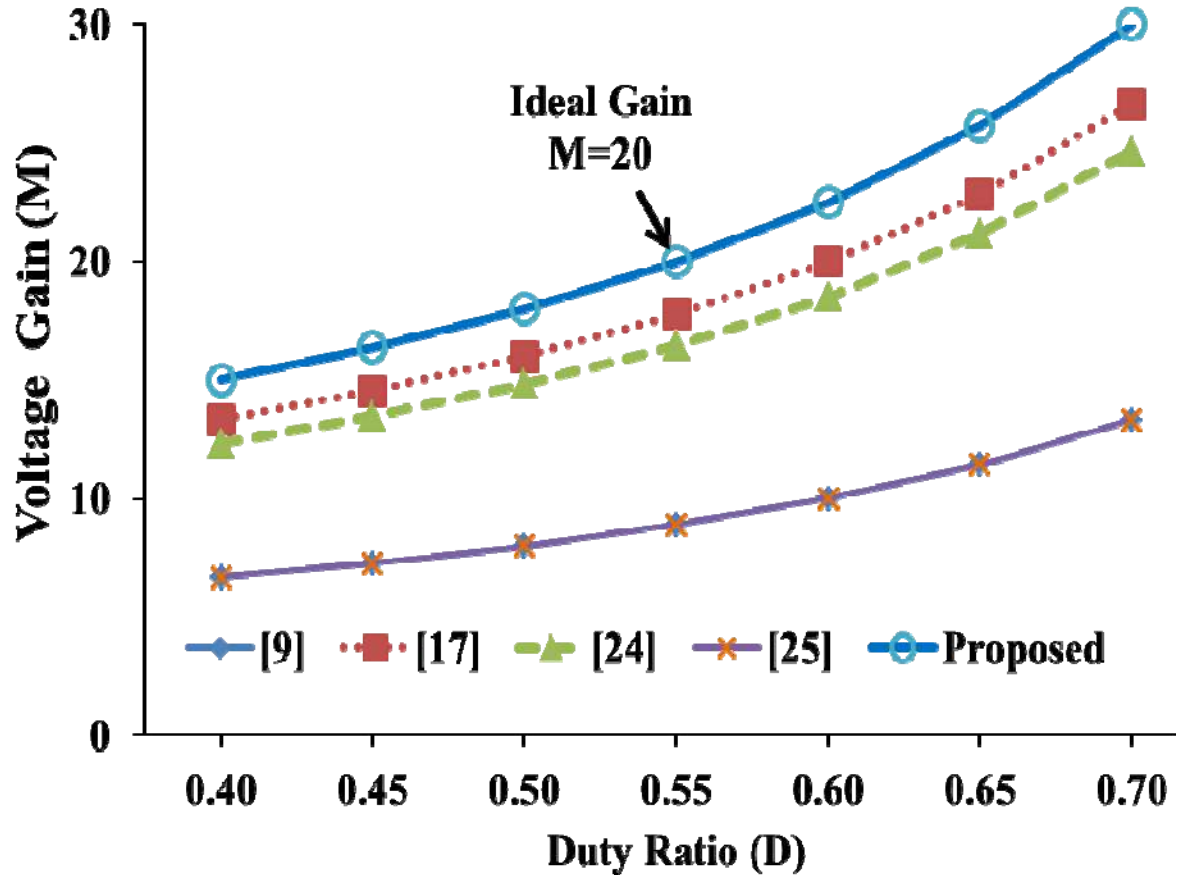
30
20
10
0
Voltage Gain (M)
Ideal Gain
M=20
[9]
[17]
[24]
[25]
Proposed
0.40
0.45
0.50
0.55
0.60
0.65
0.70
Duty Ratio (D)

(b)

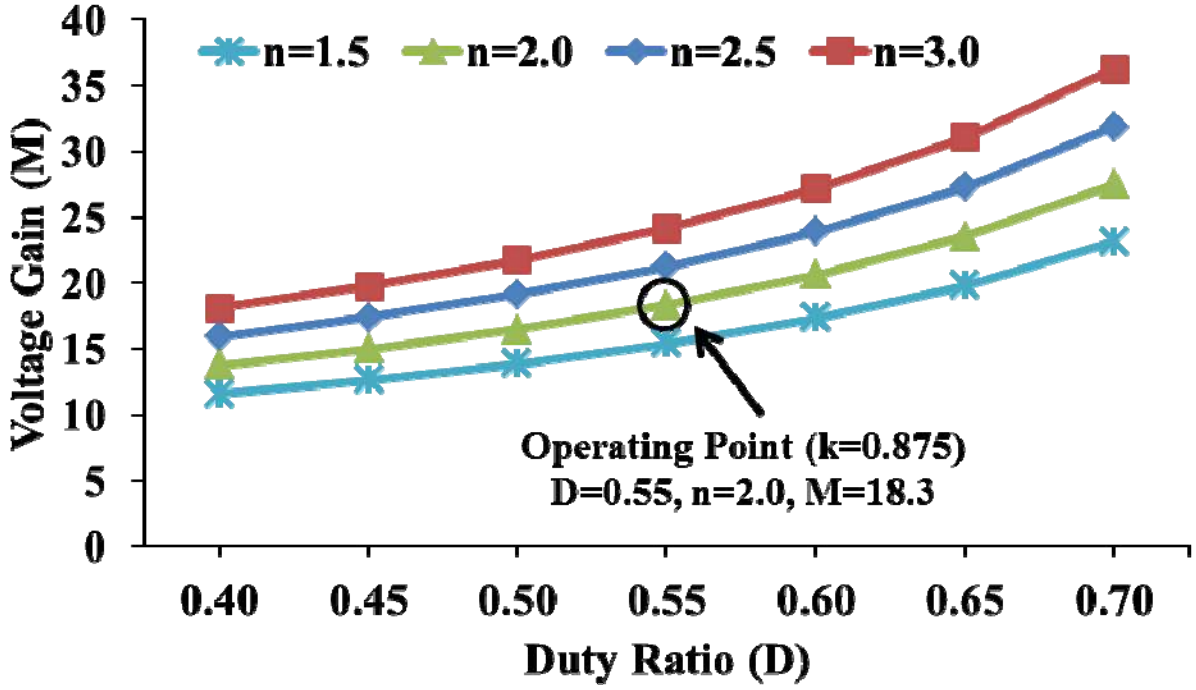
40
35
30
25
20
15
10
5
0
Voltage Gain (M)
n=1.5
n=2.0
n=2.5
n=3.0
Operating Point (k=0.875)
D=0.55, n=2.0, M=18.3
0.40
0.45
0.50
0.55
0.60
0.65
0.70
Duty Ratio (D)

(c)

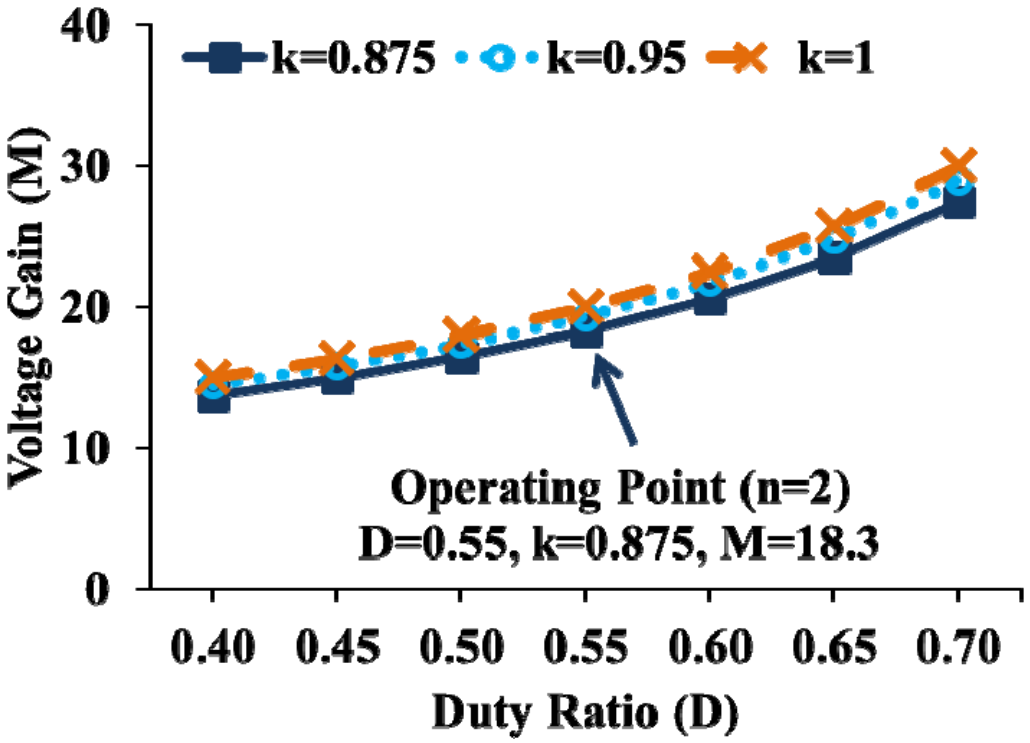

(d)

Fig. 10. Plots representative of the main performance indicators of the proposed converter

(a) Efficiency and output voltage of the proposed converter under simulation and experimentation.

(b) Voltage gain plot of the proposed converter and some existing converters when $k = 1$.

(c) Voltage gain variation of the developed converter for various values of n.

(d) Voltage gain variation of the developed converter for various values of k.

4.1.1 Switch Stress

In the proposed converter, the voltage stress experienced by Z_1 and Z_2 is 36% while Z_3 experiences a very low voltage stress of only about 12% of the output voltage. This reduced switch voltage stress is attributed to Stage 2 where the majority of gain extension takes place. Switches used in [52] and [55] experience a stress of about half of their output voltage while

in [53], the switching stress is about one-fourth of the output. In [56], switches are subjected to the least voltage stress of 12.5% of its output voltage due to clamping technique adopted.

4.1.2 Component Count

Proposed converter has maximum components and converter in [52] uses the least number of components. The presence of more components in the presented converter is acceptable since higher voltage gain, and power transfer of 3kW is simultaneously achieved. In [56], additional switches are used to reduce the voltage stress on the main switches resulting in increased component count. Other converters presented in Table 2 have a moderate component count.

Table 2. Comparison of proposed HGHP DC-DC converter with some converters proposed in the scientific literature [52]-[56].

Attributes	Converters presented in				
	[52]	[53]	[55]	[56]	Proposed
Input voltage (V_{in})	24	60	36	15	60
Output voltage (V_0)	380	590	400	200	1100
Voltage gain (M)	15.83	9.83	11.11	13.33	18.33
Output power (kW)	0.5	0.87	1	0.4	3
Duty ratio (D)	0.56	0.615	0.67	0.65	0.55
Magnetic components used	2 CI	2CI	2 CI	3CI	3 CI
CI turns ratio (n)	1.6	1	1	2	2
Generalised voltage gain expression with coupling coefficient $k = 1$	$\frac{4n+1}{1-D}$	$\frac{3n+1}{1-D}$	$\frac{4}{1-D}$	$\frac{4n}{1-D}$	$\frac{3(1+nk)}{1-D}$
Gain extension technique	CI, diode capacitor stages	Interleaved, three winding CI and VMC	Switched Capacitors, CI	Interleaved, CI, and voltage quadrupler	Interleaved, lift capacitor, CI and VMC
Expression for maximum voltage stress on power switch	$\frac{V_0}{4n+1}$	$\frac{V_{C_r}}{n}$	$\frac{V_0}{2}$	$\frac{V_o}{4n}$	$\frac{V_0}{1+nk}$
Switch stress (% of V_0)	51.35	24.4	50	12.5	36.36
No. of switches	2	2	4	6	3
No. of diodes	4	8	0	4	10
No. of capacitors	5	5	4	7	8
Total component count	13	16	14	20	23

4.3 MPPT Implementation

The proposed HGHP DC-DC converter is designed to be used in DC microgrid applications, one of the main applications is interfacing PV systems. Consequently, the converter should be able to perform additional functionalities as Maximum Power Point Tracking (MPPT). To facilitate easy implementation of a MPPT algorithm, the relation between the duty ratio (D), equivalent resistance (seen by the source) at maximum power point ($R_{Conv\text{-}MPP}$) and load resistance (R_L) is provided in (27).

$$D = 1 - \left(3 + 3nk\right)\sqrt{\frac{R_{Conv-MPP}}{R_L}} \tag{27}$$

5 Challenges

Although DC microgrid has bright opportunities and is the right candidate to encounter the future energy demand by integrating DG and the loads, some challenges are associated while implementing a DC distribution scheme [58]. Some of the main challenges are discussed below.

(i) The use of high DC bus voltages of the order of 1 kV is more attractive at distribution levels as they reduce the current and copper weight. However, when DC bus voltage exceeds 75 V, additional safety measures are required to avoid electrocution [59] – [62]. Apart from proper electrical insulation, an active protection system is also required to detect insulation failures, leakage currents, etc., and to isolate the power supply and loads. Though designing a complete safety system for DC is difficult, other safety mechanisms like residual current detector (RCD) and insulation resistance monitoring device (IMD) guarantee the necessary safety and monitoring functions.

(ii) The growth of DC distribution is constrained due to lack of higher current interrupting capacity of DC circuit breaker (CB), protection schemes and operational experience. However, expert research on fault detection and protection of DC distribution system has resulted in advanced protection schemes which are capable of investigating different faults and prove to be effective for DC distribution system with distributed energy sources [63] – [66].

(iii) When DC distribution is carried out through underground (UG) cables in urban areas, corrosion is likely to be more compared to AC [67].

(iv) Though there are different arguments towards the voltage levels and standards, to reach a breakthrough, standardisation of voltage levels is an important step. Organisations like Emerge Alliance (EA), the European Telecommunications Standards Institute (ETSI), the International Electrotechnical Commission (IEC) and IEEE are actively involved in evolving and fixing the appropriate policies and standards.

(v) Manufacturing of DC compatible appliances is still in a nascent stage. Industries which manufacture products for DC distribution systems are very few since the demand for DC compatible loads/appliances is very low. On the other hand, minor modifications can be done in the present appliances or devices to make them "DC-ready" [68] – [70].

6 Prospects

Despite some stiff challenges, DC microgrids and DC distribution, in particular, have wider implications on efficient energy utilisation. The motivation to encounter the challenges may be obtained by looking at some of the bright prospects that DC distribution is expected to offer. Some of the ways to easily shift/adapt towards DC distribution are as follows:

(i) Present AC distribution lines can be upgraded into DC with few minor infrastructure changes resulting in increased power transfer capacity [71].

(ii) In residential and commercial buildings, it is standard practice to install multiple wiring networks for lighting loads, ring mains, the internet, intercom, etc., Therefore, adding a supplementary DC electrical network is perfectly achievable [72]. Further, DC sockets can be provided at modest cost. Introducing DC lines in residences will increase the market demand for DC appliances. Resultantly, they will keep getting better, and a wider range of products that work in DC will come into existence. In the long run, this phenomenon is expected to make DC appliances more affordable and efficient.

(iii) In longer time perspective, smaller communities may find that their off-grid DC microgrid systems more reliable and satisfy their needs [73]. The quality of the power delivered to the customer will be improved. Further, as the distance between the generating station and load centre comes down drastically, the utility bills will also be reduced.

Therefore, DC distribution has (i) a prosperous future, (ii) the potential to efficiently and effectively replace the existing AC system and (iii) provide reliable and high-quality power at a much affordable cost.

7 Conclusion

A high gain high power DC-DC converter suitable for DC microgrid, considering integration of PV system is developed. A non-isolated DC-DC converter has been developed to simultaneously realise high voltage gain at a higher power level for DC microgrid applications. When the converter is supplied from a 60 V input, the converter yielded 1.1 kV at the output terminals and delivered 3 kW of power at 92.6% efficiency. Many key

performance attributes of the proposed converter has been compared with some existing converters in order to highlight the versatility of the presented converter. When fed from a RES, the benefits of DC distribution systems, key challenges involved in adapting to DC and prospects have been thoroughly discussed. Further, the efficiency at which DC distribution systems and DC microgrids supply modern loads combined with the ease of integrating DG and storage elements makes the overall concept appealing. As an extension, a DC microgrid setup can be made to operate in a smarter way viz; avoiding brownouts and or blackouts, taking care of critical loads and other load demands depending upon the source availability by incorporating intelligence and internet connectivity. Standardisation of voltage levels, safety, protection and other key issues like DC compatible appliance manufacturing, creating awareness among the consumers, installation, operation and availability of qualified and trained technicians with experience in DC distribution systems should be addressed.

8 Acknowledgement

This work is carried out with a seed fund granted by VIT University, Chennai.

9 References

[1] Yonghong Kuang, Yongjun Zhang, Bin Zhou, Canbing Li, Yijia Cao, Long Zeng. A review of renewable energy utilization in islands. Renewable and Sustainable Energy Reviews 2016; 59: 504-513.

[2] D.O. Akinyele, R.K.Rayudu, N.K.C.Nair. Global progress in photovoltaic technologies and the scenario of development of solar panel plant and module performance estimation-Application in Nigeria. Renewable and Sustainable Energy Reviews 2015; 48: 112–139.

[3] Mariya Soshinskaya, Wina H.J. Crijns-Graus , Jos van der Meer, Josep M. Guerrero. Application of a microgrid with renewables for a water treatment plant. Applied Energy 2014; 134: 20–34.

[4] D.O. Akinyele , R.K. Rayudu. Community-based hybrid electricity supply system: A practical and comparative approach. Applied Energy 2016; 171:608–628.

[5] G.D. Kamalpur, R.Y. Udaykumar. Rural electrification in India and feasibility of photovoltaic solar home systems. Electrical Power and Energy Systems 2011; 33: 594–599.

[6] Peng Zhang, Wenyuan Li, Sherwin Li, Yang Wang, Weidong Xiao. Reliability assessment of photovoltaic power systems: Review of current status and future perspectives. Applied Energy 2013; 104:822–833.

[7] Estefanía Planas, Jon Andreu, José Ignacio Gárate, Iñigo Martínez de Alegría, Edorta Ibarra. AC and DC technology in microgrids: A review. Renewable and Sustainable Energy Reviews 2015; 43:726–749.

[8] R. K. Chauhan, B. S. Rajpurohi, S. N. Singh, and F. Gonzalez-Longatt. DC Grid Interconnection for Conversion Losses and Cost Optimization. Chapter 14, In Green Energy and Technology Series, Renewable Energy Integration: Challenges and Solutions, Springer-Verlag 2014; 327-345.

[9] G. Pandey, S. N. Singh, B. S. Rajpurohit, and F. M. Gonzalez-Longatt. Smart DC Grid for Autonomous Zero Net Electric Energy of Cluster of Buildings. IFAC-Papers on Line 2015; 48(30): 108-113.

[10] F. Gonzalez-Longatt, B. S. Rajpurohit, J. L. R. Torres, and S. N. Singh. Simulation platform for autonomous smart multi-terminal DC micro-grid. IEEE Innovative Smart Grid Technologies - Asia (ISGT-Asia) 2016; 630-635.

[11] K. Chauhan, B. S. Rajpurohit, R. E. Hebner, S. N. Singh, and F. Gonzalez-Longatt. Voltage Standardization of DC Distribution System for Residential Buildings. Journal of Clean Energy Technologies 2016; 4(3):167-172.

[12] Mariya Soshinskaya, Wina H.J. Crijns-Graus, Josep M. Guerrero, Juan C. Vasquez. Microgrids: Experiences, barriers and success factors. Renewable and Sustainable Energy Reviews 2014; 40:659–672.

[13] Vahid Mortezapour, Hamid Lesani. Hybrid AC/DC microgrids: A generalized approach for autonomous droop-based primary control in islanded operations. Electrical Power and Energy Systems 2017; 93:109–118.

[14] Rasmus Luthander, Joakim Widén, Daniel Nilsson, Jenny Palm. Photovoltaic self-consumption in buildings: A review. Applied Energy 2015; 142: 80–94.

[15] Lidula N.W.A, Rajapakse.A.D. Microgrids research: a review of experimental microgrids and test systems. Renewable and Sustainable Energy Reviews 2011;15: 186-202.

[16] Jackson John Justo, Francis Mwasilu, Ju Lee, Jin-Woo Jung. AC-microgrids versus DC-microgrids with distributed energy resources: A review. Renewable and Sustainable Energy Reviews 2013; 24: 387–405.

[17] R. Noroozian, M. Abedi, G.B. Gharehpetian, S.H. Hosseini. Distributed resources and DC distribution system combination for high power quality. Electrical Power and Energy Systems 2010;32: 769–781.

[18] Ahmed T. Elsayed, Ahmed A. Mohamed, Osama A. Mohammed. DC microgrids and distribution systems: An overview. Electric Power Systems Research 2015; 119:407–417.

[19] Laurens Mackay, Tsegay Hailu, Laura Ramirez-Elizondo, Pavol Bauer. Towards a DC Distribution System – Opportunities and Challenges. IEEE First International Conference on DC Microgrids (ICDCM), 2015; 215-220.

[20] Abdullah S. Emhemed, Graeme M. Burt. Protecting the last mile – enabling an LVDC distribution network [dissertation]. University of Strathclyde; 2013.

[21] A. Bracale, P. Carmia, G. Carpinelli, E. Mancini, F.Mottola. Optimal control strategy of a DC micro grid. Electrical Power and Energy Systems 2015; 67: 25–38.

[22] Aditya Shekhar, Epameinondas Kontos, Laura Ramírez-Elizondo, Armando Rodrigo-Mor, Pavol. Bauer Grid capacity and efficiency enhancement by operating medium voltage AC cables as DC links with modular multilevel converters. International Journal of Electrical Power & Energy Systems 2017; 93:479–493.

[23] Iván Patrao n, Emilio Figueres, Gabriel Garcerá, Raúl González-Medina. Microgrid architectures for low voltage distributed generation. Renewable and Sustainable Energy Reviews 2015; 43:415–424.

[24] Rajendra Singh and Krishna Shenai. DC Microgrids and the Virtues of Local Electricity. 6 Feb 2014, http://spectrum.ieee.org/green-tech/buildings/dc-microgrids-and-the-virtues-of-local-electricity.

[25] Claes Rytoft. Data centers. ABB Review. The corporate technical journal 2013; 4(13):1-84.

[26] Venkat Rajaraman, Uma Rajesh, Prabhjot Kaur, Ashok Jhunjhunwala. Economic Analysis of deployment of DC power and Appliances along with Solar in urban multi-storied buildings. IEEE First International conference on DC Microgrids 2015.

[27] Brock Glasgo, Inês Lima Azevedo, Chris Hendrickson. How much electricity can we save by using direct current circuits in homes? Understanding the potential for

electricity savings and assessing feasibility of a transition towards DC powered buildings. Applied Energy 2016;180:66–75.

[28] Vagelis Vossos, Karina Garbesi, Hongxia Shen. Energy savings from direct-DC in U.S. residential buildings. Journal of Energy and Buildings 2014; 68: 223–231.

[29] Ashok Jhunjhunwala - Innovative Direct-Current Microgrids to Solve India's Power Woes – India Energy Storage Alliance Newsletter - February 2017 print issue as "The People's Grid."- http://www.indiaesa.info/index.php/iesa-industry-news/535-innovative-direct-current-microgrids-to-solve-india%E2%80%99s-powerwoes.html.

[30] D.O. Akinyele, R.K. Rayudu, N.K.C. Nair. Development of photovoltaic power plant for remote residential applications: The socio-technical and economic perspectives. Applied Energy 2015; 155:131–149.

[31] Erdal Irmak, Naki Guler. Application of high efficient voltage regulation system with MPPT algorithm. Electrical Power and Energy Systems 2013; 44(1):703–712.

[32] M.H. Taghvaee, M.A.M.Radzi, S.M.Moosavain, Hashim Hizam, M.Hamiruce Marhaban. A current and future study on non-isolated DC–DC converters for photovoltaic applications. Renewable and Sustainable Energy Reviews 2013;17: 216-227.

[33] B.Sri Revathi and M.Prabhakar. Non-isolated high gain DC-DC converter topologies for PV applications – A comprehensive review. Renewable and Sustainable Energy Reviews 2016; 66: 920-933.

[34] European Commission. Low voltage directive LVD 73/23/EEC. European commission directive: Brussels, 1973.

[35] Lohjala, J., Kaipia, T., Lassila, J., Partanen, J., Järventausta P., Verho P. Potentiality and effects of the 1kV low voltage distribution system. In proceedings of the FPS Conference 2005.

[36] Kaipia, T., Lassila, J., Partanen, J., Lohjala, J. Principles and tools for the 20/1/0.4 kV distribution network planning. In proceedings of the NORDAC Conference 2006.

[37] Lohjala, J., Kaipia, T., Lassila, J., Partanen, J. The three voltage level distribution using the 1000 V low voltage system. In proceedings of the CIRED Conference 2005.

[38] T. Kaipia, P. Salonen, J. Lassila, and J. Partanen. Possibilities of the low voltage DC distribution systems. Presented at the NORDAC 2006 Conference, Stockholm, Sweden, Aug. 2006.

[39] Yuan-mao Ye, Ka Wai Eric Cheng. Quadratic boost converter with low buffer capacitor stress. IET Power Electronics 2014;7(5):1162-1170.

[40] Wuhua Li and Xiangning He. Review of Non isolated high-step-up DC/DC converters in photovoltaic grid-connected applications. IEEE Transactions on Industrial Electronics 2011; 58(4):1239-1250.

[41] Fernando Lessa Tofoli, Dênis de Castro Pereira, Wesley Josias de Paula, Demercil de Sousa Oliveira Júnior. Survey on non-isolated high-voltage step-up DC–DC topologies based on the boost converter. IET Power Electronics 2015; 8(10):2044-2057.

[42] Musbahu Muhammad, Matthew Armstrong, and Mohammed A. Elgendy. A non-isolated interleaved boost converter for high-voltage gain applications. IEEE Journal of Emerging and Selected Topics in Power Electronics 2016; 4(2):352-362.

[43] Sheng-Yu Tseng, Chih-Yang Hsu. Interleaved step-up converter with a single-capacitor snubber for PV energy conversion applications. Electrical Power and Energy Systems 2013; 53: 909–922.

[44] Rui Ling, Guoyan Zhao, Qin Huang. High step-up interleaved boost converter with low switch voltage stress. Electric Power Systems Research 2015; 128: 11–18.

[45] Huawu Liu, Haibing Hu, Hongfei Wu, Yan Xing, and Issa Batarseh. Overview of high-step-up coupled-inductor boost converters. IEEE Journal of Emerging and Selected Topics in Power Electronics 2016;4(2):689-704.

[46] Antônio Alisson Alencar Freitas, Fernando Lessa Tofoli, Edilson Mineiro Sá Júnior, Sergio Daher, Fernando Luiz Marcelo Antunes. High-voltage gain DC-DC boost converter with coupled inductors for photovoltaic systems. IET Power Electronics 2015; 8(10):1885–1892.

[47] Xuefeng Hu and Chunying Gong. A high voltage gain DC–DC converter integrating coupled-inductor and diode–capacitor techniques. IEEE Transactions on Power Electronics 2014; 29(2): 789-800.

[48] Tohid Nouri, Seyed Hossein Hosseini, Ebrahim Babaei, Jaber Ebrahimi. A non-isolated three-phase high step-up DC–DC converter suitable for renewable energy systems. Electric Power Systems Research 2016; 140:209–224.

[49] Y Kuo-Ching Tseng, Chi-Chih Huang, and Chun-An Cheng. A single-switch converter with high step-up gain and low diode voltage stress suitable for green power-source conversion", IEEE Journal of Emerging and Selected Topics in Power Electronics, vol. 04, no. 2, pp. 363-372, Jun. 2016.

[50] Xuefeng Hu and Chunying Gong. A high gain input parallel output series DC-DC converter with dual coupled inductors. IEEE Transactions on Power Electronics 2015; 30(3):1306-1307.

[51] S. Khosrogorji, M. Ahmadian, H. Torkaman, S. Soori. Multi-input DC/DC converters in connection with distributed generation units – A review. Renewable and Sustainable Energy Reviews 2016; 66:360–379.

[52] Hadi Moradi Sizkoohi, Jafar Milimonfared, Meghdad Taheri, Sina Salehi. High step-up soft-switched dual-boost coupled-inductor-based converter integrating multipurpose coupled inductors with capacitor-diode stages. IET Power Electronics 2015; 8(9):1786–1797.

[53] Tohid Nouri, Seyed Hossein Hosseini, Ebrahim Babaei, Jaber Ebrahimi. Interleaved high step-up DC–DC converter based on three-winding high-frequency coupled inductor and voltage multiplier cell. IET Power Electronics 2015; 8(2):175–189.

[54] He, L.; Liao, Y. An advanced current auto balance high step up converter with a multi-coupled inductor and voltage multiplier for a renewable power generation system. IEEE Transactions on Power Electronics 2016; 31(10):6992 – 7005.

[55] Yi-Feng Wang, Li-Kun Xue, Cheng-Shan Wang, Ping Wang, and Wei Li. Interleaved high-conversion-ratio bidirectional DC–DC converter for distributed energy-storage systems — circuit generation, analysis, and design. IEEE Transactions on Power Electronics 2016; 31(8):5547 -5561.

[56] Yihua Hu, Weidong Xiao, Wuhua Li, Xiangning He. Three-phase interleaved high-step-up converter with coupled-inductor-based voltage quadrupler. IET Power Electronics 2014; 7(7):1841–1849.

[57] B. Sri Revathi, M. Prabhakar. High gain high power non-isolated DC-DC converter for renewable energy applications. IEEE Int. Conf. on Electric. Energy Syst. (ICEES) 2014: 229–234.

[58] IEC 60364-7-712(2002-05): Electrical installations of buildings-Part 7-712: requirements for special installations or locations-Solar photovoltaic (PV) power supply systems.

[59] IEC61140 (2001-10): Protection against electric shock-Common aspects for installation and equipment.

[60] IEC60364-1 (2001-08): Electrical installations of buildings-Part1:Fundamental principles, assessment of general characteristics, definitions.

[61] IEC61200-413 (1996-03): Electrical installation guide-Part 413: Protection against indirect contact-Automatic disconnection of supply.

[62] Y. Yu. Intelligent distribution network in the new situation. Power System and Clean Energy 2009; 25(7): 1–3.

[63] X. Feng, L. Qi, and J. Pan. Fault inductance based protection for DC distribution systems. In Proceedings of 13th Int. Conf. Develop. Power Syst. Protection, Edinburgh, Scotland 2016; 1–6.

[64] Shimin Xue, Chaochao Chen, Yi Jin,1 Yongli Li, Botong Li, and Ying Wang. Protection for DC Distribution System with Distributed Generator. Journal of Applied Mathematics 2014;1-12. http://dx.doi.org/10.1155/2014/241070.

[65] Jae-Do Park, Jared Candelaria. Fault Detection and Isolation in Low-Voltage DC-Bus Microgrid System. IEEE Transactions on Power Delivery 2013; 28(2):779-87.

[66] Jae-Do Park, Jared Candelaria, Liuyan Ma, Kyle Dunn. DC Ring-Bus Microgrid Fault Protection and Identification of Fault Location. IEEE Transactions on Power Delivery 2013; 28(2):2574-84.

[67] Dimitris Antoniou, Antonios Tzimas, Simon M. Rowland. Transition from alternating current to direct current low voltage distribution networks. IET Generation, Transmission and Distribution 2015; 9(12):1391–1401.

[68] L. Mackay, L. Ramirez-Elizondo, and P. Bauer. DC ready devices - Is redimensioning of the rectification components necessary? 16th International Conf. on Mechatronics - Mechatronika (ME) 2014; 1–5.

[69] G. Makarabbi, V. Gavade, R. Panguloori, and P. Mishra. Compatibility and performance study of home appliances in a DC home distribution system. IEEE Int. Conf. on Power Electron. Drives and Energy Syst. (PEDES) 2014: 1–6.

[70] Miguel A. Rodríguez-Otero and Efraín O'Neill-Carrillo. Efficient Home Appliances for a Future DC Residence. Energy 2030 Conference, 2008.

[71] Larruskain D, Zamora I, Abarrategui O, Aginako Z. Conversion of AC distribution lines into DC lines to upgrade transmission capacity. Electric Power System Research 2011; 81(7):1341-1348.

[72] Cemal Keles, Abdulkerim Karabibe, Murat Akcin, Asim Kaygusuz, Baris Baykant Alagoz, Ozan Gul. A smart building power management concept: Smart socket applications with DC distribution. Electrical Power and Energy Systems 2015; 64: 679–688.

[73] Emil Nyholm, Joel Goop, Mikael Odenberger, Filip Johnsson. Solar photovoltaic-battery systems in Swedish households – Self consumption and self-sufficiency. Applied Energy 2106; 183:148–159.